Automated Vessel Boundary Detection Using 3D Expansion of Dynamic Programming

Da-Chuan Cheng* Prof
http://mrt.cmu.edu.tw/english/faculty.html
Department of Biomedical Imaging and Radiological Science
China Medical University
Taichung, TW

Shing-Hong Liu Prof
http://csie.cyut.edu.tw/~shliu/
Department of Computer Science and Information Engineering
Chaoyang University of Technology
Taichung, TW

Abstract

In this paper we apply the 3D expansion of **DP** (dynamic programming) to find a near optimal surface in a 3D matrix. This algorithm can detect boundaries in an image sequence such as B-mode sonographic images and MRI sequences. We test and modify this algorithm using real B-mode **CCA** (common carotid artery) dynamic sonographic image sequences and **FA** (femoral artery) MRI sequences. The automated results are compared with experts' manual tracing results. The average error of intima detection is around 0.5 pixel (two sequences, 164 total images) and the relative error rate for vessel cross-sectional area computation in MRI is $2.8\% \pm 2.2\%$ on 6 MRI sequences (300 total images). The results demonstrate the better qualitative performance than the 2D DP.

1 Introduction

Many image edge detection methods have been proposed in the last two decades [5, 6]. Edge detection methods allow broken or discontinuous edge lines. Boundary detections, however, are somehow different, as some applications do not allow discontinuous boundaries. Many types of methods can handle the vessel extraction problem. Several hundred papers are surveyed in [3], which consider vessel extraction mainly in two-dimensional images. DP is an optimization tool often used in boundary detection [4]. The motivation of this study is raised from the observation that the femoral artery in the cross-sectional view in MRI sequences without contrast injection is sometimes invisible. The artery is visible if the blood flow velocity is large enough that it appears in contrast compared to the surrounding tissue. If the blood flow velocity is small during a short time period, the artery has limited contrast and is not visible. Under this extreme situation, the 2D DP fails to detect its boundary because it is hard to obtain a feature, normally the gray-level gradient, to represent the boundary.

To solve this problem, we have found a literature proposed by [2], which is a 3D-expansion of DP that can seek an optimal surface in a 3D matrix. The significance of this

paper is two-fold: 1) we modify the cost function in the 3D-expansion of DP so that this algorithm is able to find a closed contour and garantees the start and end points are connected; 2) we test this algorithm on the vessel boundary detection on real medical image sequences, and its unsigned relative error is reported. The results show that the proposed method is qualitatively better than the traditional 2D DP.

2 Methods

2.1 2D dynamic programming

DP is suitable for boundary detection in noisy images, including sonography [1, 4] and MRI vessel segmentation without a contrast injection. However, the drawback of 2D DP is that it does not consider the relatioship between 2 subsequent images. Therefore, if one or two images in an image sequence were blurred, 2D DP fails to detect correct boundaries in these blurred images.

2.2 3D expansion of dynamic programming for closed contour detection

The real 3D DP needs tremendous computations. This is however not practical. The main idea of 3D expansion of DP is to use some constraints to limit the computation time. At the same time, the continuities in 3D are still considered. However, the original paper [2] does not consider the connection between the start and end points if it processes the closed contour. In this paper, we modify this drawback and add an extra term in the cost function to fix this problem.

Let the 3D matrix R have size $M \times N \times P$, where M and N are the numbers of rows and columns, and P denotes its depth. The volumetric matrix contains feature image sequences of interest. Values in R are normalized, i.e., $0 \leq R(y,x,z) \leq 1$ where y, x, and z are indices of the corresponding dimensions. Assume that features are saved in the 3D matrix and the goal is to find an optimal surface having the shortest path and lowest value summation from one side on the z-axis to another side with some given constraints. The typical constraint in DP controls the smoothness or continuity of the sought surface. Assume the searching direction is from $x = 1$ to $x = N$ and $z = 1$ to $z = P$. Two parameters control the smoothness: $d_1 \geq |y_x - y_{x-1}|$ controls the smoothness on the $x-y$ plane $N \times M$, and $d_2 \geq |y_z - y_{z-1}|$ controls the smoothness on the $x-z$ plane $N \times P$. The parameters allow the maximum distance between two connected nodes. The y-coordinate $(y(x,z))$ denotes the height of the optimal surface, which can be found via an optimization problem:

$$y^*_{x,z} = \arg\min_{y_{x,z}} \sum_{x=1}^{N} \sum_{z=1}^{P} \{R(y_{x,z}) | 1 \leq x \leq N,\ 1 \leq z \leq P\}, \tag{1}$$

subject to some constraints $d_1 \geq |y_x - y_{x-1}|$ and $d_2 \geq |y_z - y_{z-1}|$;
This optimization problem minimizes the iterative cost functions as such:

$$C_1(y,x,z) = \min_{i \in (-d_1, d_1)} (C_1(y+i, x-1, z) + \beta_1 |i| + \frac{\gamma |y+i-y_0|}{N-x+1}) + R(y,x,z), \tag{2}$$

for $1 \leq x \leq N,\ 1 \leq z \leq P$. The term with a weighting factor γ is added to modify the algorithm so that it garantees the connection between the start and end point if this algorithm processes

the closed contour. The weighting factor γ can be set to 1 for closed contour detection and $\gamma = 0$ for other cases. After C_1 is fully constructed, C_2 is constructed afterward as follows:

$$C_2(y,x,z) = \min_{i\in(-d_2,d_2)}(C_2(y+i,x,z-1)+\beta_2|i|)+C_1(y,x,z), \tag{3}$$

for $1 \le z \le P,\ 1 \le x \le N$;
where C_1 and C_2 are accumulation matrices of size $M \times N \times P$. The initializations of C_1 and C_2 are thus:

$$\begin{aligned} C_1(*,1,z) &= R(*,1,z) && \text{for } 1 \le z \le P; \\ C_2(*,x,1) &= C_1(*,x,1) && \text{for } 1 \le x \le N. \end{aligned}$$

Notably, the accumulation matrices C_1 and C_2 are accumulated on y-x plane and y-z plane, respectively. The matrix C_1 must be done before C_2 starts to be computed. We found that [2] does not explain how to preserve the continuity in the y-x plane. In order to preserve the constraint $d_1 \ge |y_x - y_{x-1}|$, we make a modification: another 3D matrix C_3 is built. The matrix C_3 is built backwards from the last y-x plane ($z = P$) to the first y-x plane ($z = 1$) and the near optimal surface is obtained line-by-line sequentially. The iterative cost function C_3 is defined as follows:

$$C_3(y,x,z) = \min_{j\in(-d,d)}(C_3(y+i,x-1,z)+\beta_1|i|+\frac{\gamma|y+i-y_0|}{N-x+1})+C_2(y,x,z), \tag{4}$$

subjected to $z = P, P-1, \cdots, 1$. The optimal index i^* can be determined by the following equation:

$$i^* = \arg\min_{i\in(-d_1,d_1)}(C_3(y+i,x-1,z)+\beta_1|i|+\frac{\gamma|y+i-y_0|}{N-x+1}), \tag{5}$$

Similarly, the optimal index is stored in a 3D matrix: $Y(y,x,z) = y + i^*$, which is a pointer indicating the node on its previous column in the y-x plane.

After the process in Eq.(4 and 5) is fully done, the line is obtained via the following process. The last line (z=P) is obtained first:

$$\hat{Y}(x,z) = \hat{y_z}, \text{if } z = P;$$

where $\hat{y_z} = \{y_1, y_2, \cdots, y_N\}_{z=P}$ is the line on the z-th y-x plane obtained by the backwards tracing on $Y(y,x,z)$, subject to $\hat{y}_z = \arg\min_y \sum_{x=1}^{N} C_2(y,x,z)$. In fact, the line $\hat{y}_{z=P}$ is obtained by searching the position where the $C_3(y^*,N,P)$ has the minimal value among the last (N-th) column of C_3 and then backwards tracing using the 3D matrix $Y(y,x,z)$ from the start point (y^*,N,P).

To retrieve the rest lines ($z < P$), the line is obtained by:

$$\hat{Y}(x,z) = \hat{y_z}, \text{if } 1 \le z < P;$$

where $\hat{y_z} = \{y_1, y_2, \cdots, y_N\}_{1\le z<P}$ is the line on the z-th y-x plane obtained by the backwards tracing on $Y(y,x,z)$, subject to $\hat{y}_z = \arg\min_{y\in\Omega} \sum_{x=1}^{N} C_2(y,x,z)$, where Ω defines the condition to satisfy: $\max|\hat{y}_z - \hat{y}_{z+1}| < d_2$. Via this structure, the near optimal surface can be obtained efficiently and the resultant y-coordinate are stored in a 2D matrix $\hat{Y}(x,z)$.

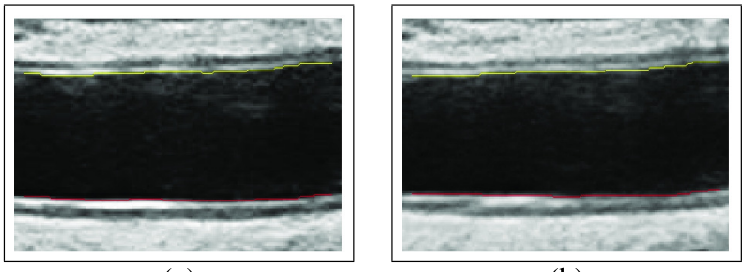

(a) (b)

Figure 1: The intima detection of near (upper line) and far walls of CCA in B-mode sonographic image sequences (S1). (Parameter setting: $\beta_1 = 0.1$, $\beta_2 = 0.05, \gamma = 0$, $d_1 = 1$, and $d_2 = 5$).

2.3 System error measurement

To estimate the error of the proposed system, two error measurements are defined as follows. They are applied for (1) CCA intima detection on B-mode sonographic image sequences (Eq.(6)) and (2) cross-sectional area of FA in MRI sequences (Eq.(7)).

Assume that the intima coordinates made by the proposed method are stored in a 2D matrix $\hat{Y}(x,z)$, $1 \le x \le N$ and $1 \le z \le P$. The manual drawing performed by experts are denoted by $\tilde{Y}(x,z)$, therefore, the error of the z-th line is defined by:

$$\varepsilon_z = \frac{1}{N} \sum_{x=1}^{N} |\hat{Y}(x,z) - \tilde{Y}(x,z)| \tag{6}$$

Assume that the cross-sectional area of the FA measured by the proposed method on the z-th image is denoted by A_z, and the manual measurement by experts is represented by $\tilde{A}_z$. Then the relative error rate (total N images) is defined by:

$$\xi = \frac{1}{N} \sum_{z=1}^{N} \frac{|Y(z) - \tilde{Y}(z)|}{\tilde{Y}(z)} \times 100 \tag{7}$$

3 Results

Two B-mode sonographic sequences are used to test. The resultant detected intima lines are shown in Fig. 1. This sequence has a larger IMT (intima-media thickness). Normally the age is a factor to influence the IMT. When IMT is increased the risk getting stroke is also increased. IMT is a clinical index in cardiovascular diseases.

Figure 2 shows a patient having a plaque in CCA. This result demonstrates the ability of the proposed system to detect intima having a plaque. The stenosis resulted from a plaque is a high risk, which causes the blood flow in a unstable way and causes turbulence.

In order to compare the manual tracing and the automated detection results, the Bland-Altman plot is modified.

The average errors (in pixel) are given in Table 1. They are around 0.5 pixel. The proposed method performs very well in detecting the intima in B-mode sonography.

We furthermore apply the method to detect the FA in MRI sequences. Due to page limitation, we have to ignore the description of MRI protocal. Table 2 shows the vessel boundary detection results of six MRI sequences. The average error rate is $2.8\% \pm 2.2\%$. All error rates are under 5%, which is acceptable for clinic measurements.

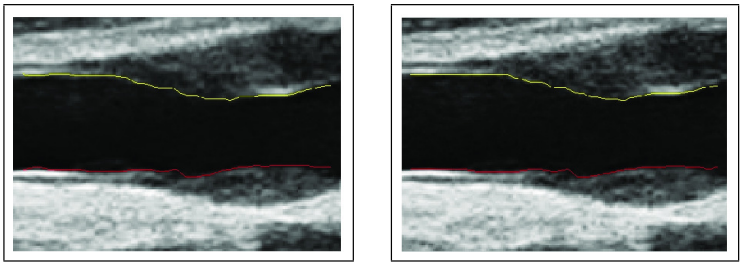

(a) (b)

Figure 2: The intima detection of near (upper line) and far walls of CCA in B-mode sonographic image sequences (S2). (Parameter setting: $\beta_1 = 0.1$, $\beta_2 = 0.05$, $\gamma = 0$, $d_1 = 1$, and $d_2 = 5$).

Table 1: The average errors in pixel.

Sequence name	Wall	Average error (pixel):Eq.(6)	Quantity of image
S1	Near wall	0.63	86
	Far wall	0.54	
S2	Near wall	0.41	78
	Far wall	0.54	

Table 2: The average error rate in percentage.

Sequence No.	Mean(%)	SD(%)
S1	2.4	1.8
S2	3.2	2.1
S3	1.4	1.3
S4	3.2	2.7
S5	3.6	2.6
S6	3.1	2.4

4 Discussions

The parameter for d_1 is normally set to 1, which implies that the boundary is smooth and no jump in an image. However, d_2 can be larger than d_1, since it allows the boundary to jump from image to image. This will happen if the artery wall moves fast especially in the dynamic B-mode sonography of CCA. However, the user does not know how much the artery wall moves, therefore, it is crucial to determine d_2. If d_2 is set too large, it might increase the computation time and more seriously is to affect the result since it might detect the wrong wall by jumping into the neighboring wall.

Our future goal is to improve this algorithm to be able to detect dual surfaces in a 3D matrix, so that the dual lines can be detected simultaneously in processing an image sequence, such as the application on the intima and adventitia detection on CCA in B-mode sonography.

5 Conclusion

We provide a modificayion on 3D DP, which garantees the connection of a closed contour. This was not noticed by the original author. Our modification performs qualitatively better than the previously published method on detection of closed contour such as the cross-sectional view of vessels either in MRI or sonography. Based on the experiments to detect the vessel boundaries in real medical images (B-mode sonography and MRI), we conclude that the propose method is able to replace the experts' manual work in vessel boundary detection.

References

[1] D.C. Cheng and Xiaoyi Jiang. Detections of arterial wall in sonographic artery images using dual dynamic programming. *IEEE Trans. on Information Technology in Biomedicine*, 12(6):792–799, 2008.

[2] D.C. Cheng and Jui-Teng Lin. Three-dimensional expansion of a dynamic programming method for boundary detection and its application to sequential magnetic resonance imaging (mri). *Sensors*, 12:5195–5211, 2012.

[3] C. Kirbas and F. Quek. Vessel extraction techniques and algorithms: a survey. In *Third IEEE Symposium on Bioinformatics and Bioengineering*, 2003.

[4] Q. Liang, I. Wendelhag, J. Wikstrand, and T. Gustavsson. A multiscale dynamic programming procedure for boundary detection in ultrasonic artery images. *IEEE Trans. on Medical Imaging*, 19:127–142, 2000.

[5] L. Zhai, S. Dong, and H. Ma. Recent methods and applications on image edge detection. In *Proceedings of the 2008 international Workshop on Education Technology and Training, 2008 international Workshop on Geoscience and Remote Sensing*, 2008.

[6] D. Ziou and S. Tabbone. Edge detection techniques: An overview. *International Journal of Pattern Recognition and Image Analysis*, 8(4):537–559, 1998.